

000
 001
 002
 003
 004 **Supplementary Material to “External Prior Guided Internal Prior Learning for**
 005 **Real Noisy Image Denoising”**
 006
 007
 008
 009
 010
 011
 012
 013
 014
 015
 016
 017
 018
 019
 020
 021
 022
 023
 024
 025
 026
 027
 028
 029
 030
 031
 032
 033
 034
 035
 036
 037
 038
 039
 040
 041
 042
 043
 044
 045
 046
 047
 048
 049
 050
 051
 052
 053

054

055

056

057

058

059

060

061

062

063

064

065

066

067

068

069

070

071

072

073

074

075

076

077

078

079

080

081

082

083

084

085

086

087

088

089

090

091

092

093

094

095

096

097

098

099

100

101

102

103

104

105

106

107

Anonymous CVPR submission

Paper ID 1047

In this supplementary material, we provide:

1. The closed-form solution of the proposed weighted sparse coding model in the main paper.
2. More denoising results on the real noisy images (with no “ground truth”) provided in the dataset [1].
3. More denoising results on the 15 cropped real noisy images (with “ground truth”) used in the dataset [2].
4. More denoising results on the 60 cropped real noisy images (with “ground truth”) from [2].

1. Closed-Form Solution of the Weighted Sparse Coding Problem (4)

The weighted sparse coding problem in the main paper is:

$$\min_{\alpha} \|\mathbf{y} - \mathbf{D}\alpha\|_2^2 + \|\mathbf{w}^T \alpha\|_1. \quad (1)$$

Since \mathbf{D} is an orthonormal matrix, problem (1) is equivalent to

$$\min_{\alpha} \|\mathbf{D}^T \mathbf{y} - \alpha\|_2^2 + \|\mathbf{w}^T \alpha\|_1. \quad (2)$$

For simplicity, we denote $\mathbf{z} = \mathbf{D}^T \mathbf{y}$. Since $\mathbf{w}_i = c * 2\sqrt{2}\sigma^2 / (\Lambda_i + \varepsilon)$ is positive (please refer to Eq. (18) in the main paper), problem (2) can be written as

$$\min_{\alpha} \sum_{i=1}^{p^2} ((\mathbf{z}_i - \alpha_i)^2 + \mathbf{w}_i |\alpha_i|). \quad (3)$$

The problem (3) is separable w.r.t. α_i and can be simplified to p^2 scalar minimization problems

$$\min_{\alpha_i} (\mathbf{z}_i - \alpha_i)^2 + \mathbf{w}_i |\alpha_i|, \quad (4)$$

where $i = 1, \dots, p^2$. Taking derivative of α_i in problem (4) and setting the derivative to be zero. There are two cases for the solution.

(a) If $\alpha_i \geq 0$, we have

$$2(\alpha_i - \mathbf{z}_i) + \mathbf{w}_i = 0. \quad (5)$$

The solution is

$$\hat{\alpha}_i = \mathbf{z}_i - \frac{\mathbf{w}_i}{2} \geq 0. \quad (6)$$

So $\mathbf{z}_i \geq \frac{\mathbf{w}_i}{2} > 0$, and the solution $\hat{\alpha}_i$ can be written as

$$\hat{\alpha}_i = \text{sgn}(\mathbf{z}_i) * (|\mathbf{z}_i| - \frac{\mathbf{w}_i}{2}), \quad (7)$$

where $\text{sgn}(\bullet)$ is the sign function.

(b) If $\alpha_i < 0$, we have

$$2(\alpha_i - \mathbf{z}_i) - \mathbf{w}_i = 0. \quad (8)$$

The solution is

$$\hat{\alpha}_i = \mathbf{z}_i + \frac{\mathbf{w}_i}{2} < 0. \quad (9)$$

So $\mathbf{z}_i < -\frac{\mathbf{w}_i}{2} < 0$, and the solution $\hat{\alpha}_i$ can be written as

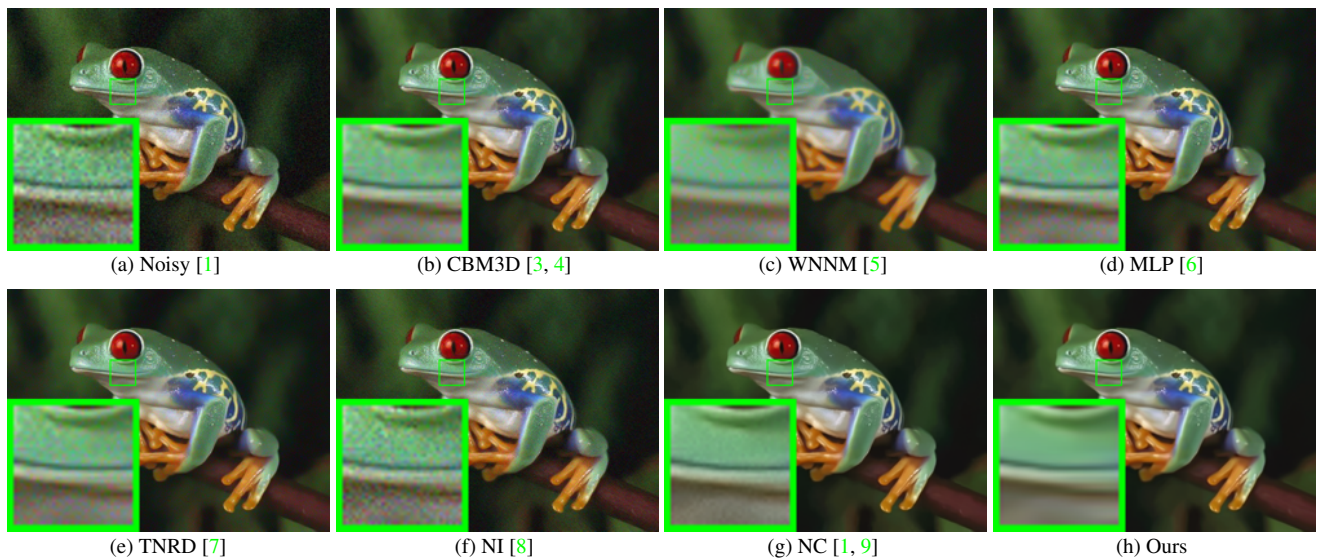
$$\hat{\alpha}_i = \text{sgn}(\mathbf{z}_i) * (-\mathbf{z}_i - \frac{\mathbf{w}_i}{2}) = \text{sgn}(\mathbf{z}_i) * (|\mathbf{z}_i| - \frac{\mathbf{w}_i}{2}). \quad (10)$$

108 In summary, we have the final solution of the weighted sparse coding problem (1) as
 109
 110 $\hat{\alpha} = \text{sgn}(\mathbf{D}^T \mathbf{y}) \odot \max(|\mathbf{D}^T \mathbf{y}| - \mathbf{w}/2, 0),$ (11)

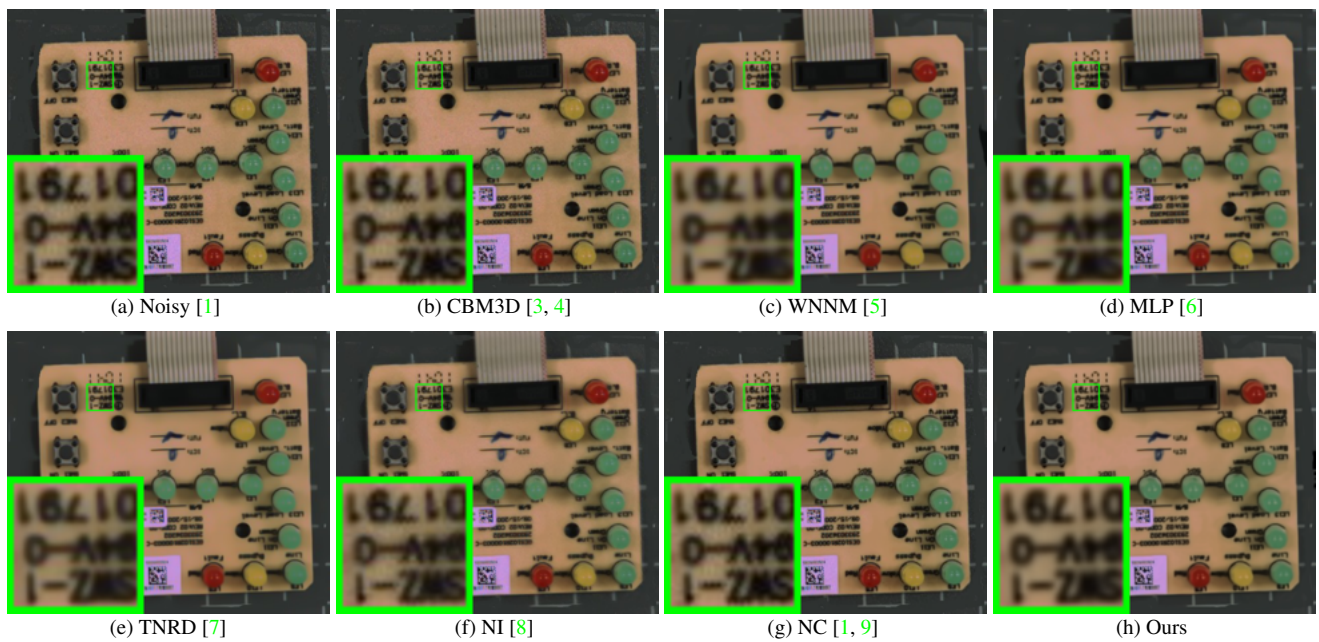
111 where \odot means element-wise multiplication and $|\mathbf{D}^T \mathbf{y}|$ is the absolute value of each entry of the vector $\mathbf{D}^T \mathbf{y}.$

112 2. More Results on Real Noisy Images in [1]

114 In this section, we give more visual comparisons of the competing methods on the real noisy images provided in [1]. The
 115 real noisy images in this dataset [1] have no “ground truth” images and hence we only compare the visual quality of the
 116 denoised images by different methods. As can be seen from Figures 1-4, our proposed method performs better than the state-
 117 of-the-art denoising methods. This validates the effectiveness of our proposed external prior guided internal prior learning
 118 framework for real noisy image denoising.
 119



138 Figure 1. Denoised images of the real noisy image “Frog” [1] by different methods. The images are better to be zoomed in on screen.
 139



161 Figure 2. Denoised images of the real noisy image “Circuit” [1] by different methods. The images are better to be zoomed in on screen.
 162



Figure 3. Denoised images of the real noisy image “Woman” [1] by different methods. The images are better to be zoomed in on screen.

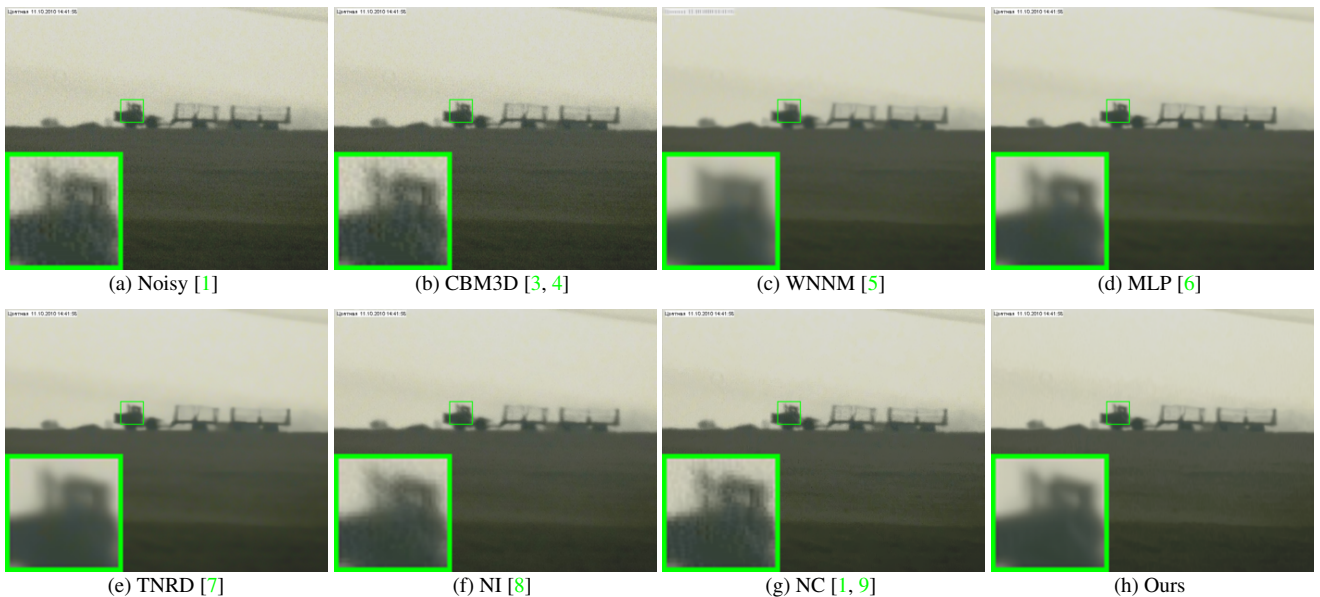
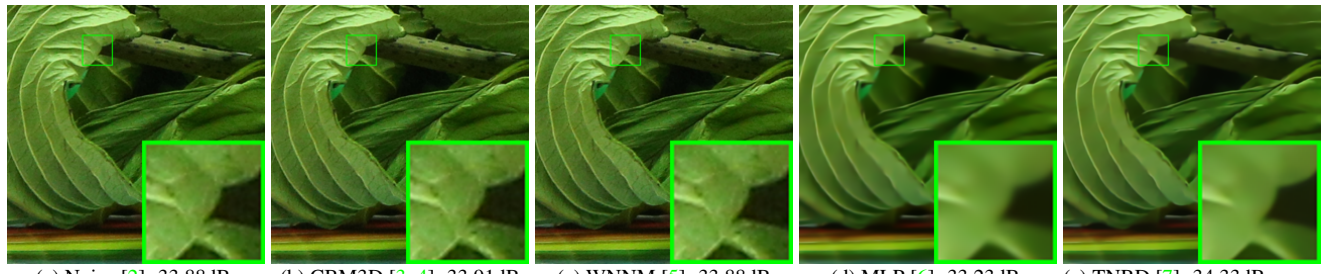


Figure 4. Denoised images of the real noisy image “Vehicle” [1] by different methods. The images are better to be zoomed in on screen.

3. More Results on the 15 Cropped Images Used in [2]

In this section, we provide more visual comparisons of the proposed method with the state-of-the-art denoising methods on the 15 cropped real noisy images used in [2]. As can be seen from Figures 5-9, on most cases, our proposed method achieves better performance than the competing methods. This validates the effectiveness of our proposed external prior guided internal prior learning framework for real noisy image denoising.

324



378

379

380

381

382

383

384

385

386

387

388

389

390

391

392

393

394

395

396

397

398

399

400

Figure 5. Denoised images of a region cropped from the real noisy image “Canon 5D Mark 3 ISO 3200 2” [2] by different methods. The images are better to be zoomed in on screen.

345



401

402

403

404

405

406

407

408

409

410

411

412

413

414

415

416

417

418

419

Figure 6. Denoised images of a region cropped from the real noisy image “Canon 5D Mark 3 ISO 3200 2” [2] by different methods. The images are better to be zoomed in on screen.

368

369

370

371

372

373

374

375

376

377

420

421

422

423

424

425

426

427

428

429

430

431

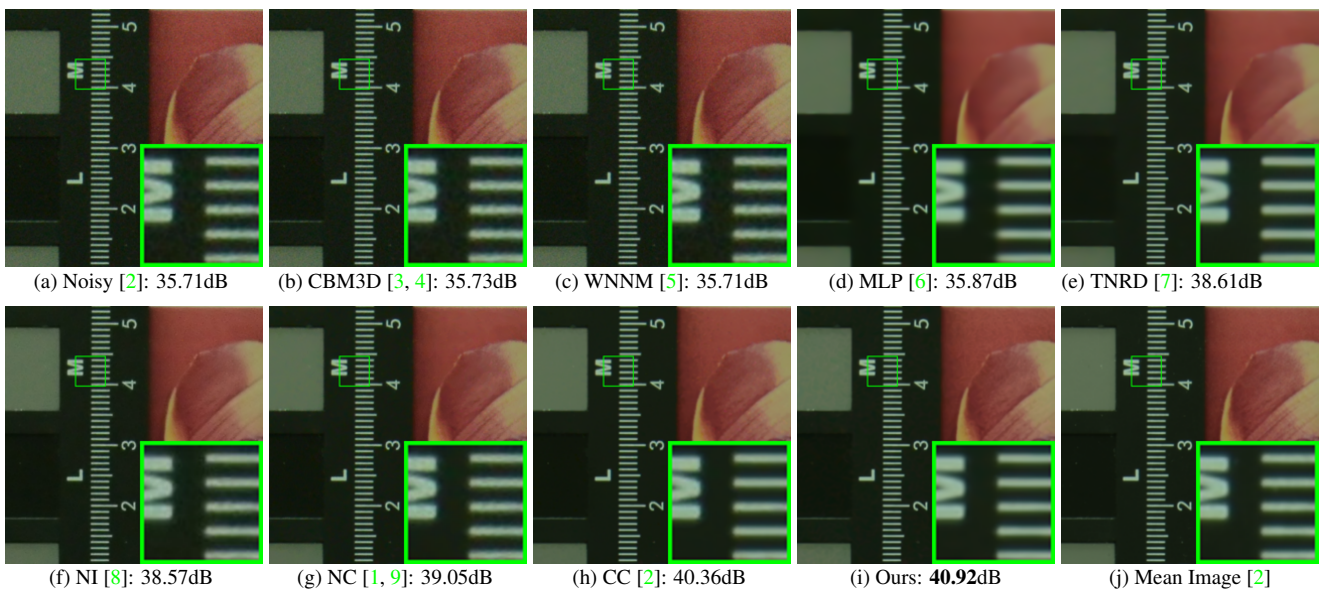


Figure 7. Denoised images of a region cropped from the real noisy image “Nikon D800 ISO 1600 2” [2] by different methods. The images are better to be zoomed in on screen.

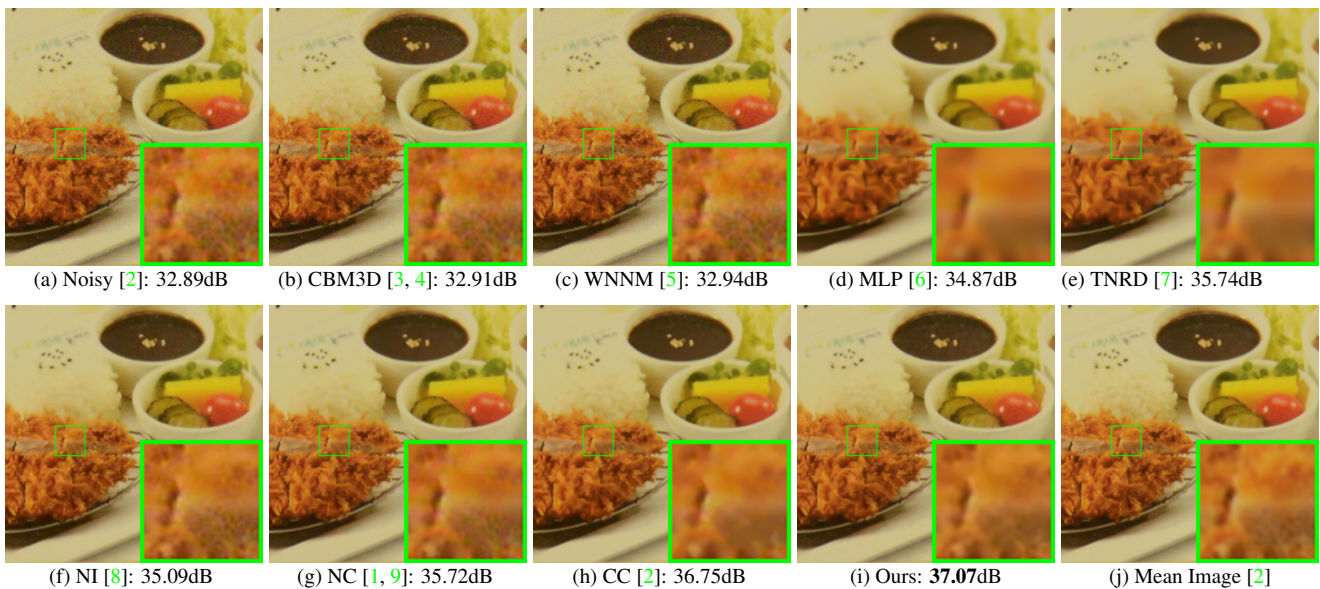


Figure 8. Denoised images of a region cropped from the real noisy image “Nikon D800 ISO 3200 2” [2] by different methods. The images are better to be zoomed in on screen.

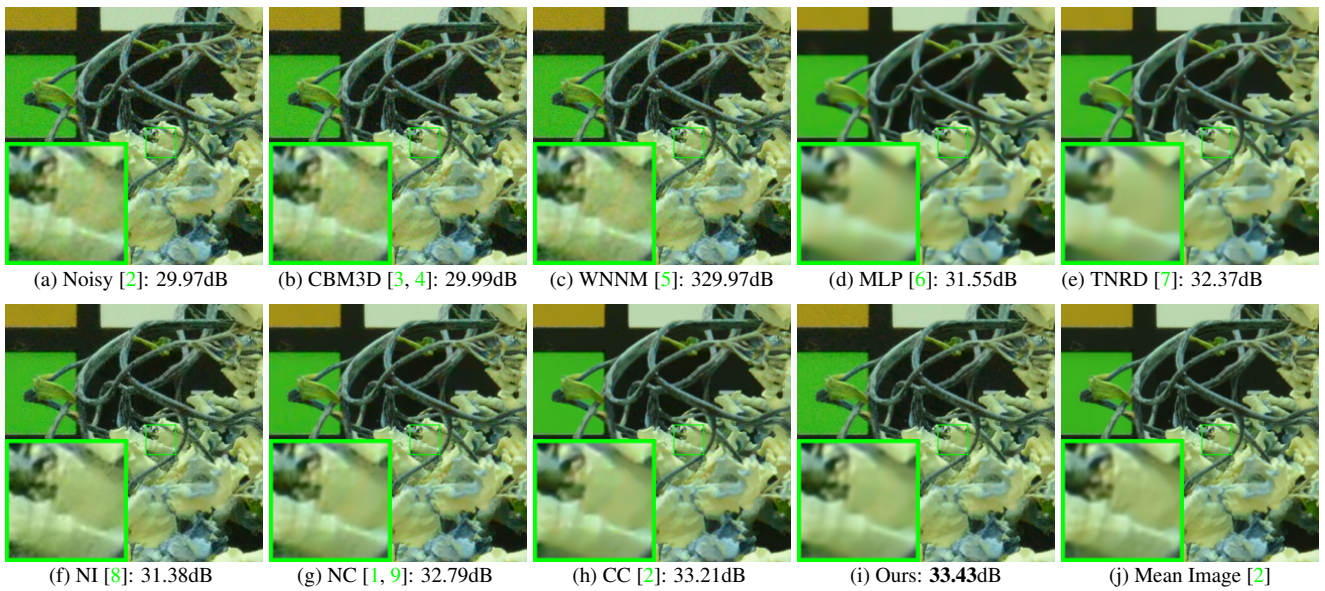


Figure 9. Denoised images of a region cropped from the real noisy image “Nikon D800 ISO 6400 2” [2] by different methods. The images are better to be zoomed in on screen.

4. More Results on the 60 Cropped Images in [2]

In this section, we provide more visual comparisons of the proposed method with the state-of-the-art denoising methods on the 60 cropped real noisy images we cropped from [2]. As can be seen from Figures 10-??, on most cases, our proposed method achieves better performance than the competing methods. This validates the effectiveness of our proposed external prior guided internal prior learning framework for real noisy image denoising.

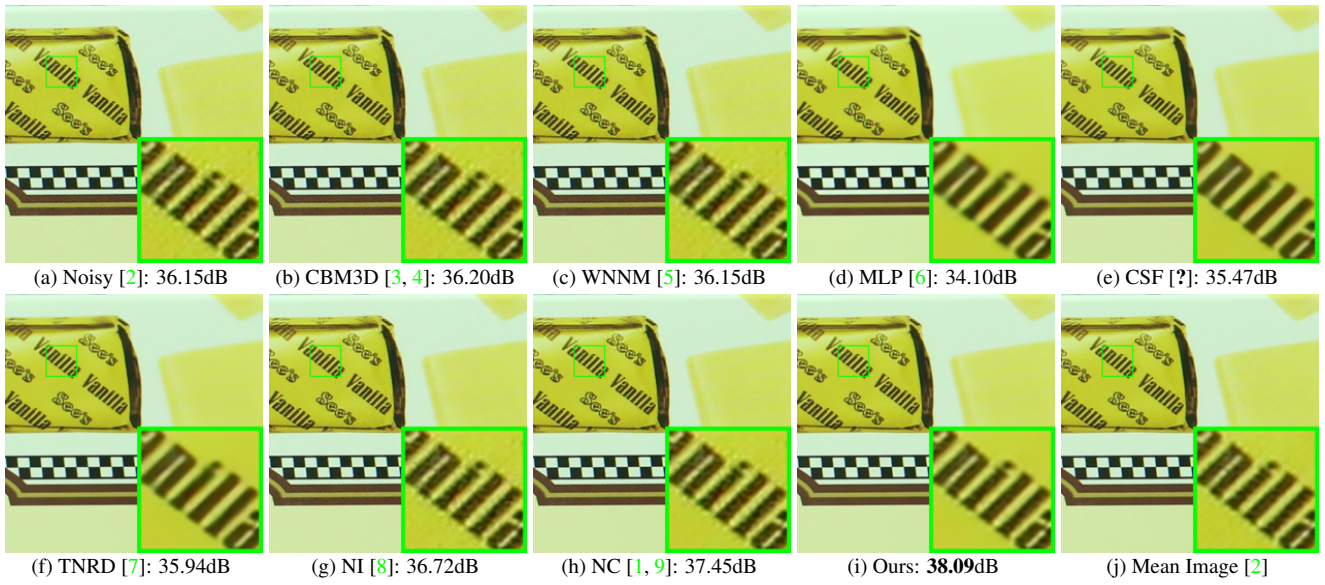


Figure 10. Denoised images of a region cropped from the real noisy image “Canon EOS 5D Mark3 ISO 3200 C1” [2] by different methods. The images are better viewed by zooming in on screen.

References

- [1] M. Lebrun, M. Colom, and J. M. Morel. The noise clinic: a blind image denoising algorithm. <http://www.ipol.im/pub/art/2015/125/>. Accessed 01 28, 2015. 1, 2, 3, 4, 5, 6

- 648 [2] S. Nam, Y. Hwang, Y. Matsushita, and S. J. Kim. A holistic approach to cross-channel image noise modeling and its application to 702
649 image denoising. *IEEE Conference on Computer Vision and Pattern Recognition (CVPR)*, pages 1683–1691, 2016. 1, 3, 4, 5, 6 703
650 [3] K. Dabov, A. Foi, V. Katkovnik, and K. Egiazarian. Image denoising by sparse 3-D transform-domain collaborative filtering. *IEEE 704
651 Transactions on Image Processing*, 16(8):2080–2095, 2007. 2, 3, 4, 5, 6 705
652 [4] K. Dabov, A. Foi, V. Katkovnik, and K. Egiazarian. Color image denoising via sparse 3D collaborative filtering with grouping 706
653 constraint in luminance-chrominance space. *IEEE International Conference on Image Processing (ICIP)*, pages 313–316, 2007. 2, 3, 707
654 4, 5, 6 708
655 [5] S. Gu, L. Zhang, W. Zuo, and X. Feng. Weighted nuclear norm minimization with application to image denoising. *IEEE Conference 709
656 on Computer Vision and Pattern Recognition (CVPR)*, pages 2862–2869, 2014. 2, 3, 4, 5, 6 710
657 [6] H. C. Burger, C. J. Schuler, and S. Harmeling. Image denoising: Can plain neural networks compete with BM3D? *IEEE Conference 712
658 on Computer Vision and Pattern Recognition (CVPR)*, pages 2392–2399, 2012. 2, 3, 4, 5, 6 713
659 [7] Y. Chen, W. Yu, and T. Pock. On learning optimized reaction diffusion processes for effective image restoration. *IEEE Conference on 714
660 Computer Vision and Pattern Recognition (CVPR)*, pages 5261–5269, 2015. 2, 3, 4, 5, 6 715
661 [8] Neatlab ABSoft. Neat Image. <https://ni.neatvideo.com/home>. 2, 3, 4, 5, 6 716
662 [9] M. Lebrun, M. Colom, and J.-M. Morel. Multiscale image blind denoising. *IEEE Transactions on Image Processing*, 24(10):3149– 717
663 3161, 2015. 2, 3, 4, 5, 6 718
664
665
666
667
668
669
670
671
672
673
674
675
676
677
678
679
680
681
682
683
684
685
686
687
688
689
690
691
692
693
694
695
696
697
698
699
700
701